JOURNAL OF PROPULSION AND POWER
Vol. 12, No. 1, January–February 1996

Transverse Jet Mixing and Combustion Experiments in Hypervelocity Flows

Jacques Bélanger*
University of Minnesota, Minneapolis, Minnesota 55455
and
Hans G. Hornung†
California Institute of Technology, Pasadena, California 91125

Transverse jet mixing and combustion experiments at a freestream velocity of 5 km/s have been conducted in the T5 free-piston shock tunnel at GALCIT. The experiments were performed in a 50 by 25 mm combustor model using a flush-mounted, Mach 1.7 single injector introducing the fuel at an angle of 15 deg relative to the main flow. The test conditions cover a range of freestream pressures from low values chosen to match previous experiments with the same duct in the HYPULSE expansion tube facility at GASL, to high pressures corresponding to the conditions closer to those in a real scramjet combustor. Tests with cold and hot hydrogen fuel were performed, the latter to better reproduce the fuel conditions of a scramjet propulsion system where the hydrogen will have to be used first as a cooling fluid. A small combustion-driven shock tunnel was used simultaneously with T5 to supply the hot fuel.

Nomenclature

d = jet exit diameter
h = enthalpy
J = momentum flux ratio, $(\rho u^2)_j/(\rho u^2)_\infty$
L_c = combustor length
M = Mach number
P = static pressure
Re_c = combustor Reynolds number, $\rho_\infty u_\infty L_c/\mu_\infty$
T = temperature
u = velocity
x = axial distance from inlet
λ = wavelength
ρ = density
ϕ = fuel equivalence ratio

Subscripts
air = T5 airflow
j = jet conditions
N_2 = T5 nitrogen flow
nom = nominal air conditions
0 = stagnation conditions
∞ = main flow conditions

Introduction

THE requirements for ground testing scramjet engines needed for an air-breathing single-stage-to-orbit vehicle are stringent. The conditions at which air enters the combustor of the engine are in the ranges of 6–18 MJ/kg for the flow total enthalpy and 40–120 kPa for the flow static pressure. But because numerical codes are not yet reliable in those flight regimes and flight tests are extremely expensive, ground-testing facilities will have to be used extensively, at least for the first phase of the engine development.

Two of the systems that can be used for this type of research are the expansion tube and the free-piston shock tunnel. Both systems have disadvantages, the free-piston shock tunnel suffers significant NO and O test gas contamination due to the high temperature reached in the nozzle reservoir, and the expansion tube has a short test time compared to the free-piston shock tunnel, significantly reducing the window of steady-state combustion regime. One of the objectives of these experiments was to compare results from T5 with those of identical tests previously made in the HYPULSE expansion tube to see if combustion differences could be detected.

While all of the previous tests done in HYPULSE used cold hydrogen injection, a small combustion-driven shock tunnel is available in T5 to supply hot hydrogen fuel for combustion experiments. To reproduce this cold fuel in some of the experiments with T5, the combustion-driven shock tunnel was converted into a Ludwieg tube with which the fuel could be supplied to the injector without increasing its temperature. Using both techniques, it was possible to compare experiments with cold and hot hydrogen injection.

Another objective for these experiments was to test the combustor at much higher static pressure. T5 can supply test gas with static pressure 2.5–3 times the maximum static pressure in the test section of HYPULSE. Because the combustion process is mostly a three-body reaction, this higher pressure can result in reaction rates increased by a factor of 6.25–9, significantly improving the ability to detect combustion. This higher static pressure is also more representative of a real flying propulsion system where the static pressure would be about 50 kPa at the flow total enthalpy used here.

Experimental Setup

The free-piston shock tunnel T5 can produce flow enthalpies between 5–25 MJ/kg at static pressures of up to 50 kPa for a test duration of approximately 1.5 ms.[1,2] According to Jacobs et al.[3] and Rogers and Weidner,[4] who have studied flow and mixing establishment time in pulse facilities using the Langley Research Center SPARK-2D code, less than 0.5 ms is needed to establish the flow inside the combustor for these test conditions.

Free-Piston Shock Tunnel T5

For the test gas to reach an enthalpy of 25 MJ/kg in the test section, the test gas must be first compressed by a 5000 m/s shock wave and subsequently stopped by the reflected

Received May 11, 1994; revision received April 17, 1995; accepted for publication April 19, 1995.
*Temporary Assistant Professor. Member AIAA.
†Clarence L. Johnson Professor of Aeronautics and Director. Member AIAA.

shock. This $M = 14-15$ shock wave, even with helium as the driver gas, cannot be generated without preheating the driver gas. For a reasonable pressure ratio between a helium driver gas and the test gas (usually air or nitrogen), e.g., less than 5000, a helium temperature of about 4000 K is needed to produce the right shock speed. This high temperature is achieved by adiabatic compression of the helium using a piston inside the driver section. Rupture of the main diaphragm occurs when the pressure inside the driver section has reached a predetermined level.

The initial length of the driver section is 30 m, but it is only of the order of 0.5 m at diaphragm rupture. The 120-kg piston is pushed inside the driver section by a 15-MPa maximum pressure air reservoir. The shock-tube section itself is 12 m long with an i.d. of 9 cm. The nozzle at the end of the shock tube has a 2.5-cm throat with an exit diameter of 30 cm.

Instrumentation

The T5 modular data acquisition system consists of 40 channels of 12-bit A/D programmable digitizer with 1-MHz maximum sampling rate. The system is controlled from a Sun SPARCstation.

The flow-visualization system is a differential interferometer using a 34-in. divergence angle Wollaston prism. The optical layout is a typical Z-shape, single-pass system with one optical table on each side of the test section. To increase the sensitivity of the system, resonant enhancement of the refractive index of the medium was used. The technique relies on the fact that the refractive index of a gas goes through a maximum very close to a spectral line of the medium. The value of the refractive index at this maximum is considerably above the broadband value. This technique was achieved in these experiments by seeding the hydrogen jet with sodium in the form of salt and using a light source with a wavelength just off to the red side of the higher energy D-line of sodium ($\lambda = 589.6$ nm). To give an idea of the increase in sensitivity, only 100 parts per billion of sodium would have to be present in the flow to get good sensitivity. The light source was a tunable dye laser built in the laboratory for that purpose. The laser is pumped by a Nd:YAG laser and can produce 40 mJ/pulse with a bandwidth of about 3 GHz. The dye used is rhodamine 610.

Combustion-Driven Shock Tunnel

The combustion-driven shock tunnel can supply hydrogen at temperatures reaching 2000 K with a total pressure of up to 25 MPa. The system minimizes the total amount of hydrogen used during a test making it a very safe method to supply the hot hydrogen. Because both T5 and the combustion-driven shock tunnel have a test time of approximately 1.5 ms, synchronization of both devices is critical. The synchronization is achieved by using a probe mounted inside the driver section of the combustion-driven shock tunnel that is in contact with the diaphragm, but electrically insulated from the rest of the tube. The probe is then used to deliver a large electrical current to the diaphragm, effectively melting it at the point of contact. This local weakening of the diaphragm is rapidly followed by its complete failure. Tests showed repeatability to within 50 μs.[5]

The combustion-driven shock tunnel was converted into a Ludwieg tube for the cold-hydrogen injection tests. To do so, the driver section of the system was used as the actual Ludwieg tube and filled with hydrogen. The driven section was left open to the test section of T5 by omitting the secondary diaphragm at the nozzle injector, leaving the driven section under vacuum before the tests. The diaphragm bursting system was used to break the main diaphragm about 3 ms before the actual test time. During these 3 ms, the hydrogen had time to fill the driven section and stabilize its pressure in the area of the nozzle injector.

Test Model

The combustor has a cross section of 50.8 by 25.4 mm and is 711 mm long. Optical windows in the model side walls permit flow visualization extending from 83 to 387 mm from the inlet of the combustor. The injector used during these tests was a Mach 1.7, flush-mounted nozzle injecting at an angle of 15 deg relative to the main flow. The injector nozzle is conical with a half angle of 1.25 deg and exits into the combustor 177-mm downstream of the inlet from the lower wall (see Figs. 1 and 2).

In all, 9 pressure transducers are mounted on the centerline of the injector wall and 10 on the centerline of the opposite wall and are shown in Fig. 2. The position of each transducer in mm from the inlet of the combustor is shown in Table 1.

Test Conditions

The combustor was tested at two different flow conditions. One reproduces the flow conditions of the HYPULSE experiments and the second one was to test a higher pressure case. For each of these conditions, air and nitrogen were used to compare combustion and noncombustion tests. Table 2 presents the reservoir and test section conditions for the HYPULSE tests and the present ones for both air and nitrogen. The concentration ratio of O_2, O, and NO by mass is also presented in Table 2 for each airflow.

For the low-pressure case, three different fuel injection conditions were tested. The first two used cold hydrogen injection and for these the combustion-driven shock tunnel was converted into a Ludwieg tube. These conditions reproduce as closely as possible the experiments done in HYPULSE

Table 1 Position in mm from the inlet of the combustor of the 19 pressure transducers

Pressure transducer no.	Injector wall	Opposite wall
1	89	63.5
2	206	144
3	236	201
4	263	252
5	318	328
6	372	379
7	422	473
8	524	575
9	600	626
10	—	676

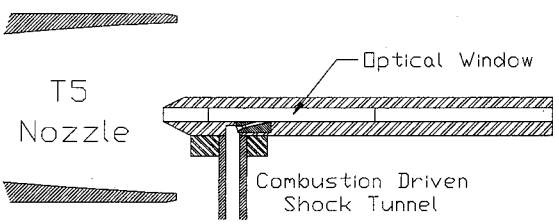

Fig. 1 Sketch of the combustor and the combustion-driven shock tunnel with respect to T5 exit nozzle.

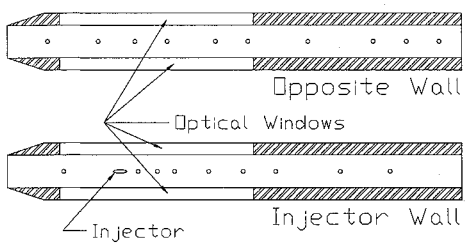

Fig. 2 Sketch of the opposite wall and injector wall of the combustor with the injector, pressure transducers, and optical window locations.

Table 2 Main flow conditions for the HYPULSE tests and for the sets of experiments done in air and nitrogen with the free-piston shock tunnel T5

Facility test gas	HYPULSE air	T5 air	T5 N_2	T5 air	T5 N_2
P_0, MPa	142	37.5	37.5	85.0	85.0
T_0, K	8350	7860	8476	8100	8875
h_0, MJ/kg	15.2	15.3	15.3	15.4	15.7
T, K	2090	2125	2015	2340	2210
P, kPa	16.5	18.3	16.8	43.9	38.5
ρ, kg/m^3	0.028	0.028	0.027	0.063	0.058
u, m/s	5060	4785	4885	4805	5005
M	5.75	5.26	5.54	5.17	5.45
Re_c, $\times 10^{-6}$	1.59	1.49	1.57	3.20	3.29
$[O_2]/[O_2]_{nom}$	0.973	0.521	—	0.672	—
$[O]/[O_2]_{nom}$	0.003	0.361	—	0.201	—
$[NO]/[O_2]_{nom}$	0.024	0.118	—	0.127	—

Table 3 Hydrogen injection conditions for the five cases studied

	T5 pressure				
	Low	Low	Low	High	High
	Nominal ϕ				
	1	2	2	1	2
	H_2				
	Cold	Cold	Hot	Hot	Hot
P_{0j}, MPa	0.41	0.79	1.5	2.4	4.8
T_{0j}, K	300	300	1250	1500	1500
P_j, kPa	83	160	305	485	970
T_j, K	190	190	790	950	950
u, m/s	1780	1780	3640	3980	3980
J	0.52	1.01	1.93	1.35	2.70
Actual ϕ	1.0	1.9	1.8	1.1	2.2

with $\phi = 1$ and 2. The third injection condition was performed with a hydrogen reservoir temperature of 1250 K with $\phi = 2$.

Experiments with $\phi = 1$ and 2 were also conducted at the high-pressure conditions. Both were performed with hydrogen at a reservoir temperature of 1500 K. Table 3 shows the injector conditions for the three sets of experiments in the low-pressure case and the two sets in the high-pressure case.

Experimental Results

Pressure Comparison with HYPULSE

Figures 3–8 show comparisons of the present experiments with those from the expansion tube HYPULSE facility in the low-pressure case with cold injection. First, results from the no-injection tests are presented in Figs. 3 and 4 for air and nitrogen flows, respectively. The agreement is good except for the first part of the combustor where very large pressure variations are found in the expansion tube experiments. These large pressure variations at the entrance of the combustor are believed to be caused by a weak oblique shock formed in the diffuser mounted at the end of the expansion tube. The diffuser is needed to increase the total enthalpy of the test gas.

A gradual pressure increase of about 12 kPa along the combustor is due to the growing boundary layer on its four walls. The freestream Reynolds number Re_c at the exit of the combustor is about 1.5×10^6. The transition Reynolds number in this case is not exactly known, but previous combustion experiments over a flat plate in T5,[5] where heat transfer gauges were mounted on the surface of the plate, have shown transition at a Reynolds number of about $1.2–1.5 \times 10^6$ for a flow enthalpy of 16 MJ/kg. Other experiments in T5[6] with a 5-deg half-angle cone have shown a freestream transition Reynolds number for a 15 MJ/kg flow to be at about 2.5×10^6. The higher transition Reynolds number in this case is due to the favorable pressure gradient on the cone. Measurements over a flat plate in the T4 free-piston shock tunnel[7] in Australia also give a transition Reynolds number of about 1.1×10^6 for a 14 MJ/kg flow. All of these experiments indicate that in the present case the boundary layer inside the combustor is mostly laminar with a possible transition in the last part of the combustor.

The set of experiments with $\phi = 1$ is compared with the HYPULSE tests in Figs. 5 and 6, Fig. 5 showing the results

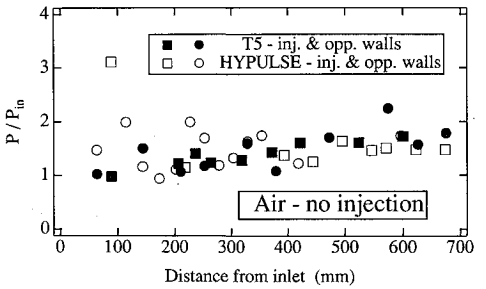

Fig. 3 Static pressure along the centerline of the injector and opposite walls for the low-pressure, no-injection case in air.

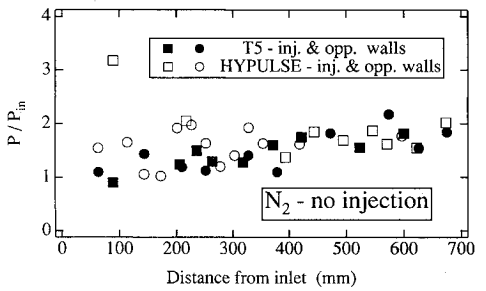

Fig. 4 Static pressure along the centerline of the injector and opposite walls for the low-pressure, no-injection case in nitrogen.

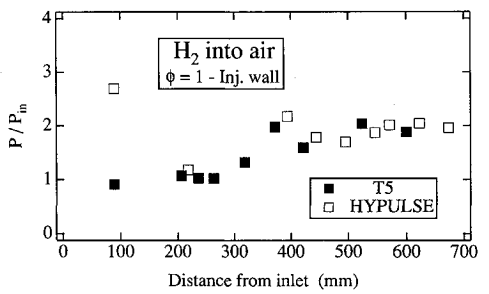

Fig. 5 Static pressure measurements on the injector wall for the low-pressure case in air with $\phi = 1$. The injector is 177 mm from the inlet.

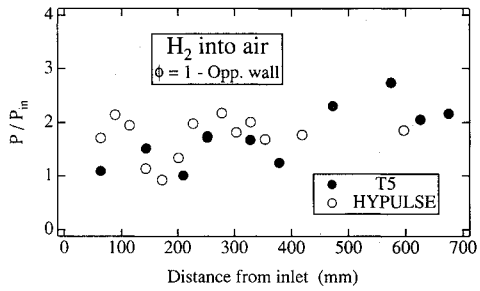

Fig. 6 Static pressure measurements on the opposite wall for the low-pressure case in air with $\phi = 1$. The injector is 177 mm from the inlet.

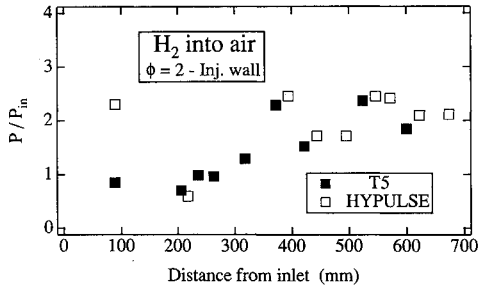

Fig. 7 Static pressure measurements on the injector wall for the low-pressure case in air with $\phi = 2$. The injector is 177 mm from the inlet.

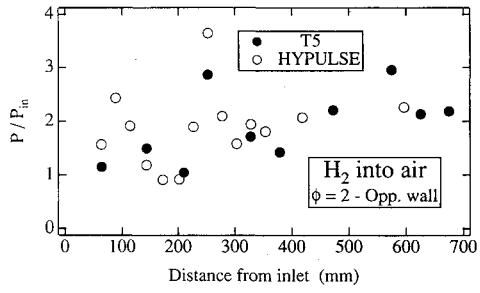

Fig. 8 Static pressure measurements on the opposite wall for the low-pressure case in air with $\phi = 2$. The injector is 177 mm from the inlet.

in air on the injector wall and Fig. 6 showing the results on the opposite wall. In the same way the sets of experiments for $\phi = 2$ are compared in Figs. 7 and 8. All of the pressure measurements presented in this section are nondimensionalized by the inlet pressure. For HYPULSE, this inlet pressure is the exit static pressure of the expansion tube and, for the present work, it is the average pressure of the two front pressure transducers. The position of the pressure transducers inside the combustor could not be reproduced exactly because the fuel had to be injected from the bottom wall of the model in the present experiments compared to HYPULSE where the fuel was injected from the top wall.

The results show excellent agreement between the present experiments and those done in the expansion tube HYPULSE. The location of the bow-shock multiple reflections was very well reproduced in the experiments. The overall pressure level was also well reproduced, except, once again, for some of the high-pressure measurements near the inlet of the combustor in the HYPULSE tests, probably caused by the weak oblique shock coming from the diffuser. The agreement between the two sets of experiments in the nitrogen cases is also excellent.

It is interesting to examine the case with $\phi = 2$ (Figs. 7 and 8). The impingement of the incident bow shock on the opposite wall (Fig. 8) at a distance of 250 mm from the inlet is very well located for these tests, as well as the first reflection of the shock on the injector wall at a distance of 375 mm from the inlet (Fig. 7). The large pressure levels measured on both walls between 500–600 mm from the inlet are believed to be caused by a side wall reflection of the bow shock.

It is necessary to say at this point that the measurement techniques available for these tests were not able to detect any effects due to the differences in the chemical composition of the freestream in the two different facilities. Any effects due to the shorter test time of HYPULSE were not detected either.

Combustion Analysis

One of the goals of these experiments has been to determine if it is possible to burn the hydrogen before it exits the combustor. To do so, combustion tests in air and noncombustion tests in nitrogen will be compared. As shown in Table 2 the static pressure in the airflow is expected to be 10% higher than that in nitrogen due to the real gas effects in the nozzle of T5. Figure 9 shows the measured pressure ratio between the air and nitrogen flow for the low-pressure case with no injection. The pressure ratio is very close to the expected value of 1.1 and stays at that level along the whole length of the combustor.

Figures 10 and 11 show the pressure ratio between air and nitrogen flows for the two sets of experiments with cold injection, Fig. 10 for the tests with $\phi = 1$ and Fig. 11 for those with $\phi = 2$. The pressure level for each of the injection conditions and for each test gas is determined using an average

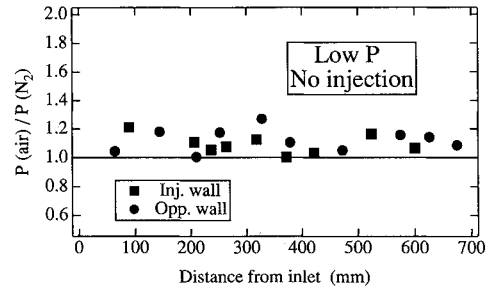

Fig. 9 Static pressure ratio between the air and nitrogen flow for the low-pressure case with no injection.

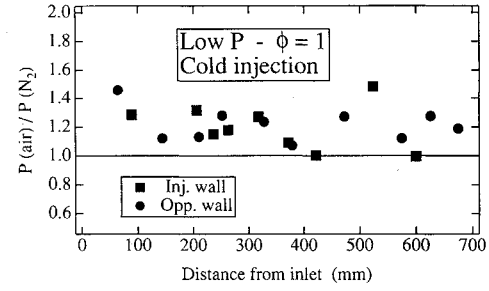

Fig. 10 Static pressure ratio between the air and nitrogen flow for the low-pressure case with cold hydrogen injection and $\phi = 1$.

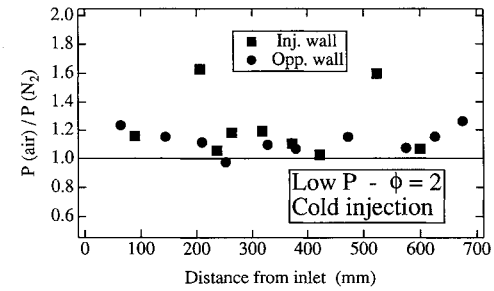

Fig. 11 Static pressure ratio between the air and nitrogen flow for the low pressure case with cold hydrogen injection and $\phi = 2$.

over two experiments. The worst case error bar for those pressure ratios is estimated at ± 0.15.

Figure 10 shows, for $\phi = 1$, a net increase from the pressure ratio of 1.1 seen in the no-injection case. It is hard to determine the pressure ratio at the exit of the combustor accurately, but an average ratio for the last third of the duct gives 1.23, which is in good agreement with Riggins et al.,[8] who ran this particular test numerically with the three-dimensional SPARK code and predicted that only 20% of the combustion would be completed after 600 mm, giving an actual pressure ratio rise of about 1.25.

Figure 11 shows the results for $\phi = 2$. The pressure ratio here can be estimated at 1.22 using again the last third of the duct for the average. This somewhat lower than expected combustion efficiency probably comes from the rather large uncertainty in the pressure measurement coupled with a small pressure rise from these combustion tests. But once again, this value of 1.22 is close to that predicted by the three-dimensional model and well within the error bars compared to the tests with $\phi = 1$. The very large pressure ratio of 1.6 measured on the injector wall at 525 mm from the inlet may indicate significant combustion in that region of the flow. This location in the combustor is just downstream of where the reflected shock impinges on the injector wall.

Figure 12 presents the pressure ratio results for the low-pressure case with $\phi = 2$ and hot hydrogen. Even if some of the pressure ratios are very high in the first part of the combustor, the ratios seem to settle rapidly to about 1.1, indicating that no significant combustion occurred in these tests. This result corroborates previous combustion experiments over a flat plate in T5 with hot fuel where higher pressure was needed to ignite the mixture at this particular enthalpy.[5]

The fact that the hydrogen temperature at the exit of the injector is almost 800 K in the hot injection case may leave the impression that it would burn much faster than in the cold injection case. But a closer look at the problem may explain why it is not the case. First, the temperature of the air behind the initial bow shock is more than 3500 K, making this temperature the dominant factor, and not the 800 K hydrogen, for the reaction rate in the flow. Second, in the hot hydrogen case, the hydrogen velocity is about 3600 m/s compared to 1800 m/s for the cold case, making the smaller velocity gradient at the interface with the 4800 m/s airflow much less effective in mixing the hydrogen. There is also a problem with the residence time of the fuel in the combustor. The hot fuel stays in the combustor only 200 μs, half the residence time of the cold fuel, making it again more difficult for the flow to mix and burn inside the combustor.

It is difficult to detect a variation of pressure of about 5 kPa due to a 20% hydrogen combustion when, at the same time, the pressure rise due to the boundary layer in the combustor is about 12 kPa. This problem is much less severe in the second set of experiments done at high pressure. With a static pressure of about 40 kPa, a 20% hydrogen combustion would cause a pressure rise of about 12 kPa, about the same as the 14-kPa rise due to the boundary layer. Another advantage is the increased density, making the combustion rate much faster. All of these high-pressure tests were done with hot hydrogen injection, making it more difficult for the combustor to burn the fuel according to the previous results, but more realistic of an actual scramjet combustor.

Figure 13 presents the pressure ratio for the no-injection tests between the air and the nitrogen flows in the high-pressure case. The results show the expected pressure ratio of 1:1. As mentioned before, and not clearly shown here, the total pressure increase along the combustor in this case is about 14 kPa. Because the freestream Reynolds number is estimated at about 3.2×10^6 at the exit of the combustor in this case, the boundary layer is most likely turbulent at least in the downstream part of the combustor.

Figures 14 and 15 show the results for the tests with ϕ of 1 and 2, respectively. The case with $\phi = 1$ shows a small pressure ratio increase compared to the no-injection case presented in Fig. 13. The pressure ratio has reached an average value of about 1.15 in the last third of the combustor. Using a simple one-dimensional heat addition model, combustion of less than 10% of the hydrogen is estimated.

The case with $\phi = 2$ presented in Fig. 15 shows a more significant pressure ratio rise. The average value of the ratio is 1.43 for the last third of the combustor, giving a 25% combustion efficiency using the one-dimensional model. This is a large percentage taking into account the fact that the fuel stays in the combustor only 200 μs. According to Dimotakis and Hall,[9] the complete combustion should take more than

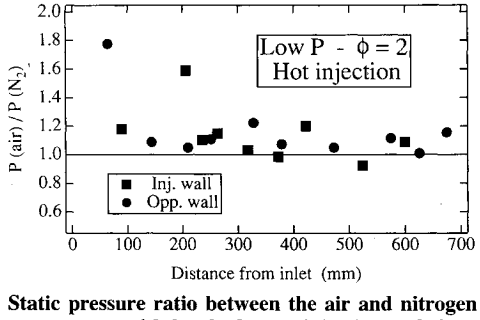

Fig. 12 Static pressure ratio between the air and nitrogen flow for the low-pressure case with hot hydrogen injection and $\phi = 2$.

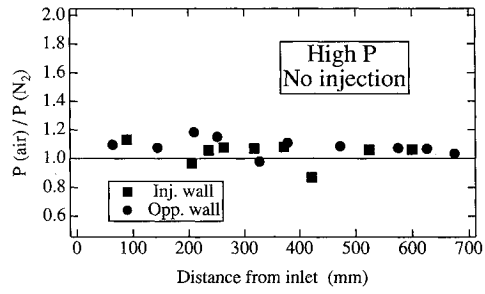

Fig. 13 Static pressure ratio for the no-injection tests in the high-pressure case, with the typical pressure ratio of 1:1 between the air and the nitrogen flows.

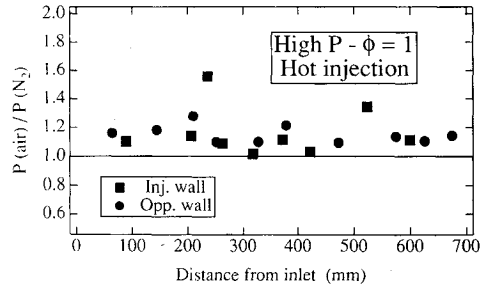

Fig. 14 Static pressure ratio between the air and nitrogen flows for the high-pressure case with hot hydrogen injection and $\phi = 1$.

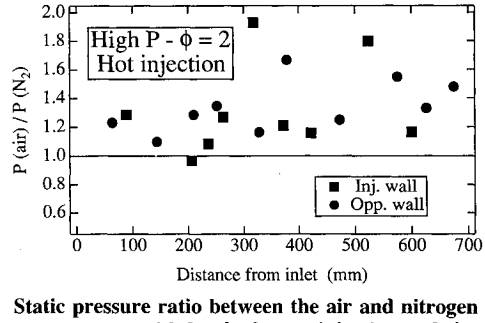

Fig. 15 Static pressure ratio between the air and nitrogen flows for the high-pressure case with hot hydrogen injection and $\phi = 2$.

1 ms. It is possible that a significant portion of this combustion occurs in the boundary layer of the combustor where the fuel has a longer residence time and where the air temperature is higher. There is also evidence in this case that some combustion occurred in the stronger bow shock region compared to the case with $\phi = 1$ (see flow visualization section).

Another point discussed by Dimotakis and Hall is the fact that for high enthalpy flows like the one tested here, the pressure and temperature rise is much smaller than that predicted by the simple one-dimensional model. This is due to a significant participation of energetic species in the final equilibrium population. It could mean that a larger percentage of the fuel actually burned than the one estimated using the one-dimensional model.

Flow Visualization

The cases presented here are first the low-pressure ones with cold injection and $\phi = 1$ and 2 in air in Figs. 16 and 17, respectively, and for the hot hydrogen case in nitrogen in Fig. 18. In all of these photographs, the bow shock and fuel penetration into the main flow are well defined. The scale of the mixing structure is also clearly evident. The reflected shock is not so well defined, probably because of three-dimensional effects. The higher penetration of the jet in Fig. 18 compared to the cold injection (Figs. 16 and 17) is due to a higher momentum of the jet at the exit of the injector.

Finally, Figs. 19 and 20 show the flow visualization for the high-pressure tests with $\phi = 2$ in air and in nitrogen, respectively. The photographs for these two higher density flows give a better resolution of the smaller scales in the flow.

Figures 19 and 20 were taken at the same delay time relative to the flow start and the stagnation conditions of the combustion-driven shock tunnel and of T5 were the same within a margin of error of 2%. Even with these similar conditions the air and nitrogen flows are clearly quite different. The penetration of the jet is much stronger in the airflow, but, most importantly, the large structures on the interface of the jet and the main flow do not show the same length scale. The nitrogen flow in Fig. 20 shows large structures with a characteristic length of about 4 mm, whereas the structures in the airflow of Fig. 19 show much smaller structure scales.

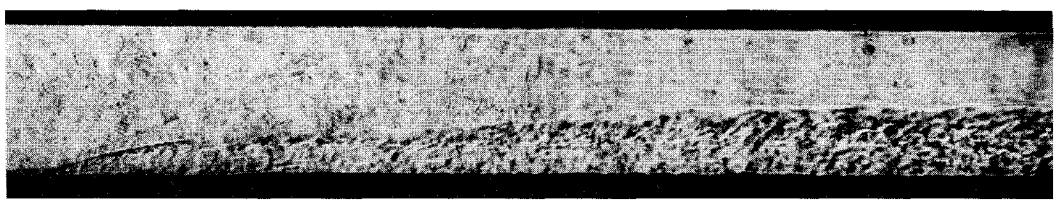

Fig. 16 Resonantly enhanced interferogram of the low-pressure case in air with cold hydrogen injection and $\phi = 1$.

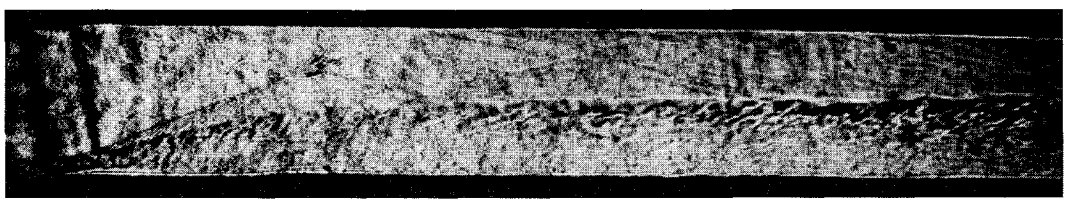

Fig. 17 Resonantly enhanced interferogram of the low-pressure case in air with cold hydrogen injection and $\phi = 2$.

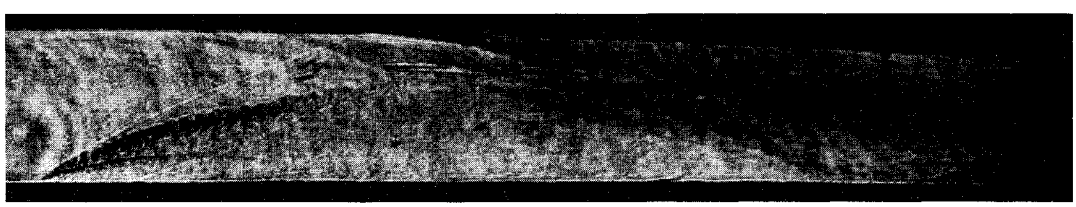

Fig. 18 Resonantly enhanced interferogram of the low-pressure case in N_2 with hot hydrogen injection and $\phi = 2$.

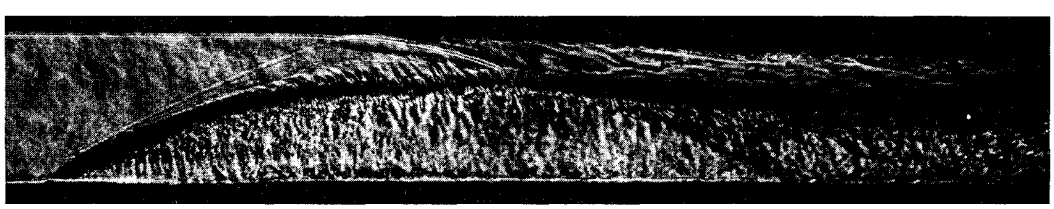

Fig. 19 Resonantly enhanced interferogram of the high-pressure case in air with hot hydrogen injection and $\phi = 2$.

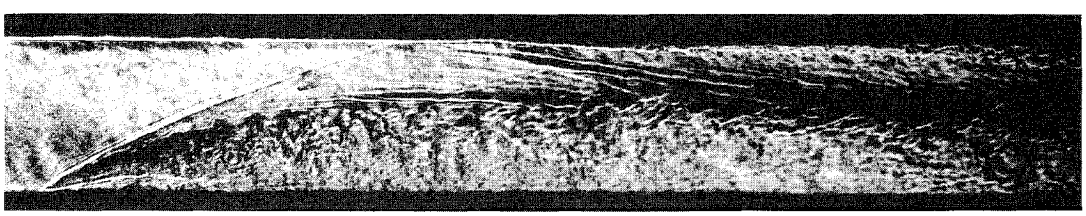

Fig. 20 Resonantly enhanced interferogram of the high-pressure case in N_2 with hot hydrogen injection and $\phi = 2$.

According to Hermanson and Dimotakis,[10] this difference in the length scale of the structures is due to a significant heat release at the interface of the jet and the main flow. For the case of a shear layer they have shown experimentally that the growth rate of the shear-layer thickness decreases with increasing heat release, and at the same time, the size of the large structures inside the shear layer decrease with respect to the shear-layer thickness as the heat release increases. These two effects add up to significantly reduce the size of the large structures for the cases where combustion occurred.

Conclusions

There is very good agreement between the HYPULSE test results and those performed in the T5 facility. No significant effects of the relatively large quantities of dissociated oxygen and NO in the T5 flow have been detected compared to the clean-air HYPULSE expansion tube flow.

It is believed that a combustion efficiency of about 20% was achieved in the low-pressure case with cold injection. In the case of the low pressure with hot injection, there is no trace of significant combustion. The combustion efficiency is estimated to have reached 25% in the high-pressure case with $\phi = 2$. The flow visualization in that case also confirms that some combustion occurred in the bow shock region of the flow. The combustion efficiency for the tests with $\phi = 1$ is significantly smaller, probably less than 10%.

Acknowledgments

This work was sponsored by the Fonds F.C.A.R. of Québec and by NASA Langley Research Center under Grant NAG-1-1209 with Clayton Rogers serving as Technical Monitor. We would also like to thank Eric Cummings for his critical work on the optical system and John I. Erdos and Jose Tamagno at GASL for their technical support and the supply of the test model.

References

[1]Hornung, H. G., Sturtevant, B., Bélanger, J., Sanderson, S., Brouillette, M., and Jenkins, M., "Performance Data of the New Free Piston Shock Tunnel T5 at GALCIT," 18th International Symposium on Shock Wave and Shock Tubes, Sendai, Japan, July 1991.

[2]Hornung, H. G., "Performance Data of the New Free Piston Shock Tunnel T5 at GALCIT," AIAA Paper 92-3943, July 1992.

[3]Jacobs, P. A., Rogers, R. C., Weidner, E. H., and Bittner, R. D., "Flow Establishment in a Generic Scramjet Combustor," *Journal of Propulsion and Power*, Vol. 8, No. 4, 1992, pp. 890–899.

[4]Rogers, R. C., and Weidner, E. H., "Scramjet Fuel-Air Mixing Establishment in a Pulse Facility," *Journal of Propulsion and Power*, Vol. 9, No. 1, 1993, pp. 127–133.

[5]Bélanger, J., "Studies of Mixing and Combustion in Hypervelocity Flows with Hot Hydrogen Injection," Ph.D. Dissertation, California Inst. of Technology, Pasadena, CA, April 1993.

[6]Germain, P., "The Boundary Layer on a Sharp Cone in High-Enthalpy Flow," Ph.D. Dissertation, California Inst. of Technology, Pasadena, CA, Nov. 1994.

[7]He, Y., and Morgan, R. G., "Transition of Compressible High Enthalpy Boundary Layer Flow over a Flat Plate," 10th Australian Fluid Mechanics Conf., Univ. of Melbourne, Australia, Dec. 1989.

[8]Riggins, D. W., McClinton, C. R., Rogers, R. C., and Bittner, R. D., "A Comparative Study of Scramjet Injection Strategies for High Mach Number Flows," AIAA Paper 92-3287, July 1992.

[9]Dimotakis, P. E., and Hall, J. L., "A Simple Model for Finite Chemical Kinetics Analysis of Supersonic Turbulent Shear Layer Combustion," AIAA Paper 87-1879, June–July 1987.

[10]Hermanson, J. C., and Dimotakis, P. E., "Effects of Heat Release in a Turbulent, Reacting Shear Layer," *Journal of Fluid Mechanics*, Vol. 199, Feb. 1989, pp. 333–375.